

Optical conductivity in non-equilibrium d -wave superconductors

J.P. Carbotte¹ and E. Schachinger^{2,*}

¹*Department of Physics and Astronomy, McMaster University,
Hamilton, Ontario, L8S 4M1 Canada*

²*Institute of Theoretical and Computational Physics
Graz University of Technology, A-8010 Graz, Austria*

(Dated: June 19, 2018)

We consider the optical conductivity of a d -wave BCS superconductor in the presence of a non-equilibrium distribution of excess quasiparticles. Two different simplified models used in the past for the s -wave case are considered and results compared. In the T^* -model of Parker the excess quasiparticles are assumed to be in a thermal distribution at some temperature T^* larger than the equilibrium sample temperature. In the μ^* -model of Owen and Scalapino a chemical potential is introduced to accommodate the excess quasiparticles. Some of the results obtained are specific to the model, most are qualitatively similar in both.

PACS numbers: 74.20.Mn 74.40.+k 74.25.Gz 74.72.-h

I. INTRODUCTION

The study of non-equilibrium superconductivity in conventional s -wave superconductors has a long history. Several comprehensive reviews exist.^{1,2,3} Much less has been done for unconventional order parameters including the high T_c oxides. The cuprates are particularly interesting since there is now a consensus that its energy gap has d -wave^{4,5,6,7} rather than s -wave symmetry. This difference is significant particularly since it implies the existence of gap nodes on the Fermi surface and hence the existence of quasiparticle states of low energies.

One might expect that quasiparticle excitations created at rather high energies through application of a laser pulse to the equilibrium sample or by some other means, would rapidly relax towards the lowest energy states available and accumulate in the nodal regions of the gap on the Fermi surface where the density of excited states goes linearly in energy. The fast relaxation processes can proceed through the electron-electron interaction which is strong in the cuprates and also through coupling to the phonons.⁸ The phonons are a separate system of excitations which can share in the excess energy provided by the excitation source. This is to be contrasted to what happens in formulations of highly correlated systems in terms of boson exchange processes,^{9,10,11,12,13,14} such as the exchange of spin fluctuations¹⁵ in the case of the Nearly Antiferromagnetic Fermi Liquid (NAFFL) model. While such exchange processes can equilibrate the energy, they do not take it out of the electronic system. Another feature of d - as opposed to s -wave non-equilibrium superconductivity is that, as has been argued by Feenstra *et al.*,¹⁶ the final stage of equilibration which proceeds through recombination of nodal quasiparticles into Cooper pairs, may take a much larger time than in s -wave because of restrictions on the kinematics. New fast laser pulse techniques^{17,18,19} have helped greatly in the study of non-equilibrium state in cuprates. These techniques have recently been used in lead¹⁸ to measure the conductivity $\sigma(T, \omega)$ under non-equilibrium conditions as

a function of frequency in the entire infrared range. Similar experiments in the cuprates should be possible and we hope this paper will stimulate such work. Here we provide a calculation of non-equilibrium effects just before recombination on the optical conductivity of a d -wave superconductor. We also consider explicitly the microwave region where analytic results can be obtained.

Very recently Nicol and Carbotte²⁰ studied the effect of a non-equilibrium distribution of quasiparticles on the gap in a BCS d -wave superconductor. In this work two well established models coming from the literature on conventional non-equilibrium superconductors are employed. These are the μ^* -model by Owen and Scalapino²¹ and the T^* -model of Parker.^{22,23} These models, while very simple, have been useful in conceptualizing what can happen, in planning, and interpreting experiments. In some sense they represent two extreme limits between which the true distribution might be expected to fall. The μ^* -model assumes that the excess quasiparticles rapidly accumulate in the lowest quasiparticle energy states available which is around the gap Δ in s -wave but is around zero in d -wave where the density of states shows a linear in energy dependence. A finite chemical potential μ^* (for the quasiparticles) is used to describe the occupation. The other extreme is to assume that the excess quasiparticles equilibrate at some new temperature T^* larger than the sample temperature T . In both cases the system is not in thermal equilibrium because the measurement is to be made before the final recombination process into Cooper pairs proceed. This is assumed to be the largest time scale in the relaxation process.

There are significant differences in behavior for d -wave as compared to s -wave. For example in terms of the excess quasiparticle density n (to be defined more precisely later) the reduction in the gap $\delta\Delta/\Delta$ is given by $-2n$ for both, T^* and μ^* models in s -wave, but for d -wave it goes like $-(4\sqrt{2}/3)\sqrt{n^3}$ for the μ^* -model and $-(32/\pi^3)\sqrt{(3n)^3}$ in the T^* model. These fundamentally different dependences on n , linear in s -wave, and to a $3/2$ power in d -wave can be simply understood. The presence

of excess quasiparticles blocks states around the Fermi surface which would otherwise be available to form the condensate in a variational sense. In d -wave, the excitations are assumed to gather around the nodal regions. In these regions the gap is small and contributes little to the condensation energy so that blocking such states is less effective than in the s -wave case where the gap is everywhere finite and equal to Δ .

In their paper Nicol and Carbotte²⁰ consider explicitly the case of tunneling in a normal-insulator-superconductor (N-I-S) junction with a non-equilibrium distribution on the superconducting side. They also address the case of pump probe experiments which claim to measure the temperature dependence of the excess quasiparticles $n(T)$ before final recombination into Cooper pairs. In the present paper we extend the work to the optical conductivity. Such calculations exist in the s -wave case²⁴ based on an appropriate generalization of the dirty limit Mattis-Bardeen formula²⁵ for the optical conductivity. Here we consider the d -wave case²⁶ and treat explicitly both, the T^* and the μ^* model and compare results obtained for the same value of excess quasiparticles n . Since in many aspects both models give the same qualitative physics, although there are some important differences which we will note, we can expect that more realistic distributions would not be so different.

In Section II we introduce some elements of the theory of the optical conductivity $\sigma(\omega, T)$ as a function of frequency ω at temperature T suitably generalized for the non-equilibrium case. In the T^* -model no formal changes to the formulas are needed, only the temperature is to be interpreted differently. In the μ^* -model all necessary changes to the mathematical formulas can be incorporated through a change of the thermal factors. In Section III we present exact numerical results for the frequency dependence of the optical conductivity (real and imaginary part) as well as for the reflectance and the normalized reflectance difference due to an excess distribution (n) of non-equilibrium quasiparticles which is the quantity that is directly measurable. Results for the T^* and μ^* -model for the same n are compared. Section IV contains a number of analytic results for a regime in which the temperature is larger than the impurity scattering rate i.e. the weak scattering limit. Comparison with exact numerical results is also given. Dependences on the excess quasiparticle density n are made explicit and helps physical understanding. A short conclusion is found in Section V. An Appendix contains some mathematical details.

II. THEORY

The non-equilibrium distribution in either T^* or μ^* -model does not change the symmetry of the gap. It does reduce its magnitude. In addition, the thermal factors which enter directly the infrared conductivity formula are also changed. These changes are modeled in one case by

the introduction of a chemical potential μ^* and in the other by simply changing the temperature from T , the temperature of the sample before application of a laser pulse, to T^* the non-equilibrium quasiparticle temperature before final recombination. For simplicity, we will assume here that the initial sample temperature T is sufficiently low that it can be considered to be zero. In the actual numerical work it is taken to be 3 K for convenience with a gap of 24 meV. For a BCS d -wave superconductor this choice corresponds to a T_c of 130 K. If we further assume that the density of excess quasiparticles n is small, we can obtain analytic results for the change in gap and for the corresponding value of μ^* and/or T^* . The necessary results are to be found in the paper by Nicol and Carbotte.²⁰ In the T^* -model $n = (\pi^2/12)(T^*/\Delta_0)^2$ and $(\delta\Delta/\Delta_0) = -(32/\pi^3)\sqrt{(3n)^2}$, while in the μ^* -model $\mu^*/\Delta_0 = \sqrt{2n}$ and $\delta\Delta/\Delta_0 = -(4\sqrt{2}/3)\sqrt{n^3}$. [From now on we will use Δ or $\Delta(n)$ for the gap with a finite n and Δ_0 for its equilibrium value when $n = 0$, i.e. $\Delta_0 = \Delta(n = 0)$.] These relationships can be used directly in our conductivity calculations. Some explanation is needed. The above results were derived for a d -wave BCS superconductor in the pure limit. To get meaningful conductivity results it is necessary to formally include some scattering mechanism. Here we will simply treat elastic impurity scattering. When this is done the impurities also formally enter the gap equation and in principle one should include these modifications along with those brought about by the non-equilibrium distribution of quasiparticles in the formula for the conductivity. Here, for simplicity, we will not do this. The impurities do reduce the size of the d -wave gap amplitude but we will assume that this is already included in our initial choice of this parameter and simply treat the changes brought about by n based on the pure case. Assuming that the impurity concentration is very small as we wish to do here, this is sufficient. There will also be a corresponding effect of impurities on the chemical potential μ^* but this is also neglected in the limit of small impurity scattering. With this explanation we can proceed with the calculation of the optical conductivity.

It is conventional, and we will follow this definition here, to measure the excess quasiparticle density n in units of $4N(0)\Delta_0$ where the factor 4 is from spin degeneracy and restricting the defining integral to positive energies only. $N(0)$ is the normal state electronic density of states at the Fermi surface. In these units

$$n = \frac{1}{\Delta_0} \left\langle \int_0^\infty d\epsilon_{\mathbf{k}} [f_T(E_{\mathbf{k}} - \mu^*) - f_T(E_{\mathbf{k}})] \right\rangle_\theta \quad (1a)$$

for the μ^* -model and

$$n = \frac{1}{\Delta_0} \left\langle \int_0^\infty d\epsilon_{\mathbf{k}} [f_{T^*}(E_{\mathbf{k}}^*) - f_T(E_{\mathbf{k}})] \right\rangle_\theta \quad (1b)$$

in the T^* -model. Here $f_T(\epsilon)$ is the usual Fermi Dirac distribution $f_T(\epsilon) = [1 + \exp(\beta\epsilon)]^{-1}$ with $\beta = 1/k_B T$ where

k_B is the Boltzmann factor which we set to one from here on. In Eqs. (1) the brackets $\langle \dots \rangle_\theta$ imply an angular average over the polar angle θ which gives the position on the Fermi surface in the two dimensional CuO_2 Brillouin zone. In terms of this angle the gap $\Delta(\theta) = \Delta \cos(2\theta)$. The quasiparticle energies $E_{\mathbf{k}} = \sqrt{\epsilon_{\mathbf{k}}^2 + \Delta^2(T, \theta)}$ where we make explicit the temperature dependence of the gap

which enters the T^* -model. Here \mathbf{k} is momentum and $\epsilon_{\mathbf{k}}$ is the normal state band energy. Consistent with our treatment of the gap equation the clean limit is used in writing down Eqs. (1).

The formula for the optical conductivity in the equilibrium case takes on the form:^{26,27,28,29}

$$\begin{aligned} \sigma(T, \nu) &= \frac{\Omega_p^2}{4\pi} \frac{i}{\nu} \left\langle \int_0^\infty d\omega \tanh\left(\frac{\beta\omega}{2}\right) [J(\omega, \nu) - J(-\omega, \nu)] \right\rangle_\theta \\ &= \frac{\Omega_p^2}{4\pi} \sigma'(T, \nu), \end{aligned} \quad (2)$$

where Ω_p is the plasma frequency and the function $J(\omega, \nu)$ is

$$\begin{aligned} 2J(\omega, \nu) &= \frac{1}{E_1 + E_2} [1 - N(\omega)N(\omega + \nu) - P(\omega)P(\omega + \nu)] \\ &\quad + \frac{1}{E_1^* - E_2} [1 + N^*(\omega)N(\omega + \nu) + P^*(\omega)P(\omega + \nu)], \end{aligned} \quad (3)$$

with $E_1^*(\omega)$, $N^*(\omega)$, and $P^*(\omega)$ the complex conjugate of $E_1(\omega)$, $N(\omega)$, and $P(\omega)$, respectively. In Eq. (2)

$$\begin{aligned} E_1(\omega) &= \sqrt{\tilde{\omega}^2(\omega + i0^+) - \tilde{\Delta}^2(\omega + i0^+)}, \\ E_2(\omega, \nu) &= E_1(\omega + \nu), \end{aligned}$$

and

$$N(\omega) = \frac{\tilde{\omega}(\omega + i0^+)}{E_1(\omega)}, \quad P(\omega) = \frac{\tilde{\Delta}(\omega + i0^+)}{E_1(\omega)}.$$

In these equations $\tilde{\omega}(\omega + i0^+)$ is the renormalized frequency which includes the impurities and in the pairing energy $\tilde{\Delta}(\omega + i0^+)$ the angular dependence on θ has been suppressed. $\sigma'(T, \nu)$ is the optical conductivity as it is calculated within our numerical programs. It is given in units of meV^{-1} . If Ω_p is given in meV then $\sigma(T, \nu)$ is given in units of meV which can easily be transformed to SI units using the relation that one $\Omega^{-1} \text{m}^{-1}$ corresponds to $5.916 \times 10^{-3} \text{meV}$. Finally, in BCS $\tilde{\Delta}(\omega + i0^+)$ is independent of ω .

To treat a non-equilibrium system a chemical potential μ^* for the excess quasiparticles is introduced in the grand canonical ensemble average and this means that the thermal factor in Eq. (2) needs to be replaced by:

$$\begin{aligned} \tanh\left(\frac{\beta\omega}{2}\right) &\longrightarrow F(\omega) \equiv [-f_T(\omega + \mu^*) \\ &\quad - f_T(\omega - \mu^*) + 1] \end{aligned}$$

while in the T^* -model there are no modifications except to change the temperature T to T^* . In Fig. 1 we compare the two factors: $F(\omega)$ and $\tanh(\omega/2k_B T^*)$ with μ^*

related to T^* by $T^* \simeq 1.56 \mu^*$. We see that both are anti-symmetric with respect to $\omega = 0$ and that $F(\omega)$ depletes the region around $\omega = 0$ more than does the hyperbolic tangent. These differences will reflex themselves in the conductivity. We begin by giving results of our numerical evaluation of Eq. (2). Before proceeding, it is necessary to specify how impurities are to be included in the theory. The impurities renormalize the frequencies to $\tilde{\omega}(\omega + i0^+)$ from ω according to the equation^{30,31}

$$\tilde{\omega}(\omega + i0^+) = \omega + i\pi\Gamma^+ \frac{\langle N(\tilde{\omega}) \rangle_\theta}{c^2 + \langle N(\tilde{\omega}) \rangle_\theta^2}, \quad (4)$$

where we have introduced the impurity scattering in a T -matrix formalism, $c = 1/(2\pi N(0)V_{imp})$. Here V_{imp} is the strength of the impurity potential and $N(0)$ the electronic density of states at the Fermi surface in the normal state which is taken to be constant, i.e. energy independent in the range of energies relevant to superconductivity. In Eq. (4) the real part of $\langle N(\tilde{\omega}) \rangle_\theta$ is the quasiparticle density of states. The parameter $\pi\Gamma^+$ is related to the impurity concentration n_I by $\pi\Gamma^+ = n_I/[N(0)\pi]$. When V_{imp} is very small $c \rightarrow \infty$, we recover the Born limit in which case we denote Γ^+/c^2 as t^+ , and for V_{imp} very large $c \rightarrow 0$ which is called the unitary limit. A realistic case would be for finite c . Fits to experimental data have given values of the order of 0.2.³¹ From the definition of c and taking $N(0)$ to be $1/W$ for $c = 0.2$, $V_{imp} \simeq 1.3W$, where W is the band width.

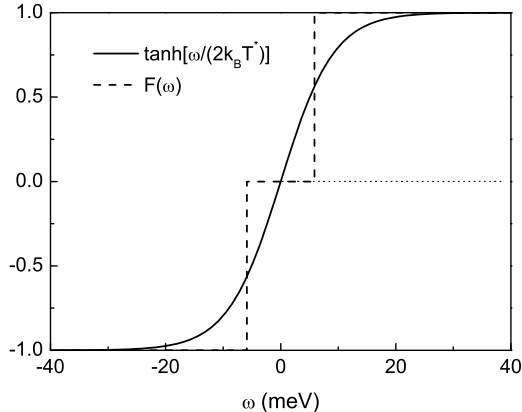


FIG. 1: The thermal factor $\tanh(\omega/2k_B T^*)$ which enters the optical conductivity (Eq. (2)) in the T^* -model (solid curve) compared with the equivalent function $F(\omega) \equiv [-\theta(\omega + \mu^*) - \theta(\omega - \mu^*) + 1]$ which enters the μ^* model (dashed curve). As shown in the text for a common value of excess quasiparticles n , $2T^* = (2\sqrt{6}/\pi)\mu^* \simeq 1.56\mu^*$. This relation is built into the figure. Here $T^* = 53$ K and $\mu^* = 5.88$ have been chosen.

III. NUMERICAL RESULTS

In the top frame of Fig. 2 we show results for the real part of the optical conductivity $\sigma'_1(\omega)$ as a function of frequency ω in computer units. To get the actual conductivity one must multiply the computer results by $\Omega_p^2/4\pi$ with Ω_p the plasma frequency. The parameters used for the run are $\Delta_0 = 24$ meV, $T = 3$ K which is low enough that it is representative of zero temperature and $t^+ = 0.1$ meV. The impurity scattering is taken in the Born limit ($c \rightarrow \infty$). The solid gray curve labeled simply by Δ_0 on the figure is the conductivity in the equilibrium limit, i.e. $n = 0$, and is included for comparison. The other four curves are with a finite non-equilibrium excess quasiparticle density of $n = 0.03$. This value of n is large compared to a value that one may realistically have in an experiment. The results obtained, however, are illustrative of what one might expect even for smaller n . For the μ^* -model $\mu^* \simeq 0.25\Delta_0$ and the change in the gap $\delta\Delta \simeq -0.01\Delta_0$ which is very small. In the T^* -model the corresponding number is $T^* \simeq 0.19\Delta_0$ and $\delta\Delta = -0.028\Delta_0$, again small but three times bigger than in the μ^* model. In the top frame of Fig. 2 the solid black and dashed curves are for $T^* = 53$ K with and without inclusion of the small gap change. We see that the direct thermal effects of T^* are much more important than any slight change in the gap. This also holds for the μ^* -model with dotted (no gap change) and dash-dotted (with gap change) curves. Comparison with the $n = 0$ case shows that the real part of the conductivity is strongly affected by the inclusion of a chemical potential $\mu^* = 5.88$ meV

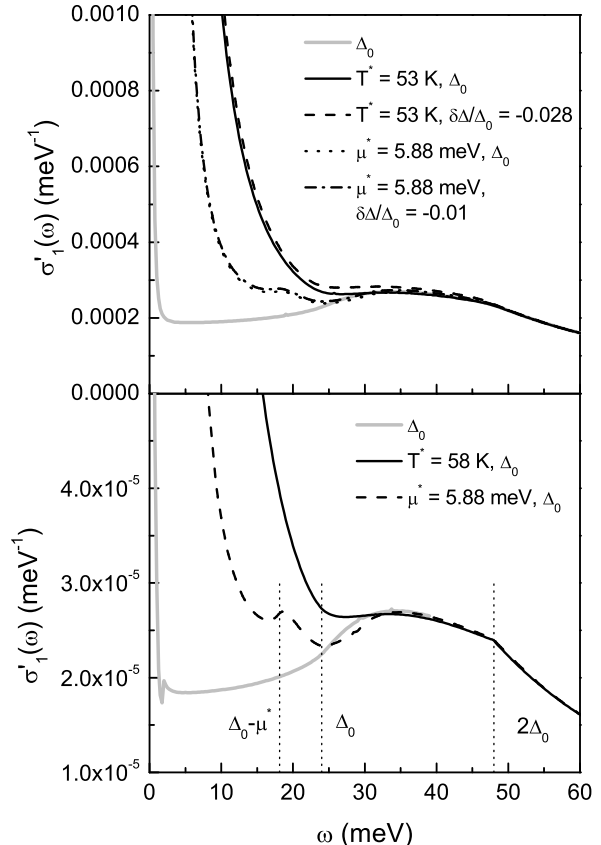


FIG. 2: Top frame: the real part of the optical conductivity $\sigma'_1(\omega)$ as a function of frequency ω . The solid gray is for the unirradiated equilibrium sample with temperature $T = 3$ K, gap $\Delta_0 = 24$ meV, and an impurity content described by $t^+ = 0.1$ meV. The solid (dashed) curve includes an excess quasiparticle density $n = 0.03$ in the T^* -model ($T^* = 53$ K) with the gap unaltered (altered to $0.972\Delta_0$). The dotted (dash-dotted) curve is for the μ^* -model ($\mu^* = 5.88$ meV) with the gap unaltered (altered to $0.99\Delta_0$). The bottom frame is the same as the top frame except that now the impurity content is greatly reduced to $t^+ = 0.01$ meV, with a single $T^* = 58$ K (solid line) and a $\mu^* = 5.88$ meV (dashed line).

and that there is significant difference between the predictions of the T^* and μ^* models. In particular, for the μ^* -model there is a distinct structure predicted to occur at the value of the gap Δ_0 minus the chemical potential μ^* . The characteristic of these structures is more easily seen in the bottom frame of Fig. 2 where additional results for $\sigma'_1(\omega)$ vs ω are given for the same gap value of 24 meV but now the impurity content is reduced by an order of magnitude to $t^+ = 0.01$ meV. The gray solid curve which applies to the equilibrium case, shows a slight change in slope at $\omega = \Delta_0 = 24$ meV as well as at $\omega = 2\Delta_0 = 48$ meV. These structures are characteristic of the logarithmic van Hove singularity in the d -wave

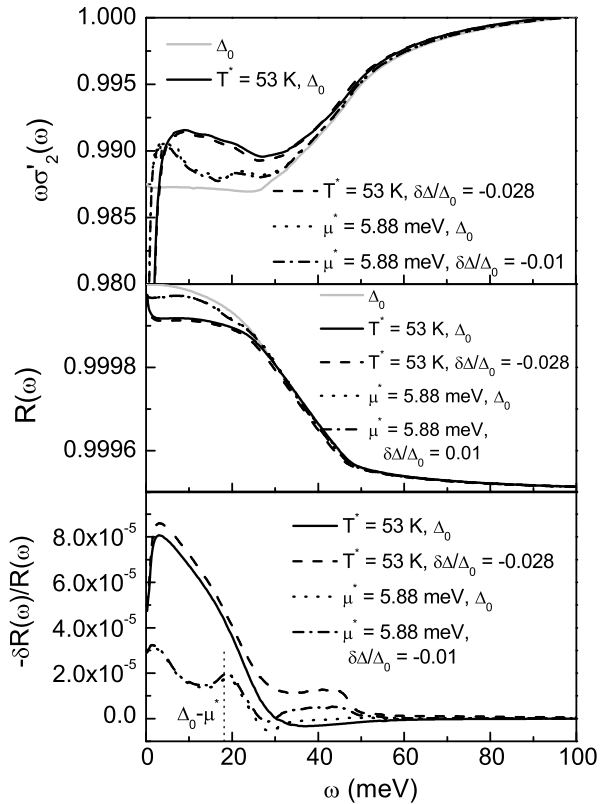


FIG. 3: Top frame: same as in the top frame of Fig. 2 except that now $\omega\sigma_2'(\omega)$ is plotted, i.e. ω times the imaginary part of the conductivity which is related to the inverse square of the penetration depth at $\omega \rightarrow 0$. Middle frame: the reflectance as a function of ω . Bottom frame: the normalized change in the reflectance $\delta R(\omega)/R(\omega)$ vs ω . To get these we have used $\Omega_p = 2$ eV and $\varepsilon_\infty = 1$.

quasiparticle equilibrium density of states. In comparison to the gray solid curve, the dashed curve which has $\mu^* = 5.88$ meV shows an additional pronounced structure at ~ 18 meV which is the value of $\Delta_0 - \mu^*$ in this case. When we also include a small shift in the gap we do see it as a small shift in the $2\Delta_0$ structure which corresponds to the smallest optical frequency which can connect both logarithmic van Hove singularities in initial and final electron state. By contrast, the structure at $\Delta_0 - \mu^*$ corresponds to a transition between the top of the occupied region of the density of states as the initial state with the van Hove singularity as the final state. The remaining curve in the bottom frame of Fig. 2 is for the T^* model (solid line). Now the region below $2\Delta_0$ is quite smooth and shows no discernible structure in contrast to the μ^* -model. This is expected since in the T^* -model the non-equilibrium distribution is assumed to be thermal.

Fig. 3 shows additional results for the case $t^+ = 0.1$ meV. In the top frame we show $\omega\sigma_2'(\omega)$ (ω multiplied by the imaginary part of the conductivity) also denoted by a frequency dependent inverse penetration

depth $\lambda_L^{-2}(\omega, T)$ in the literature. The middle frame shows the reflectance while the bottom frame shows the normalized difference in reflectance between non-equilibrium and equilibrium case, i.e. $\delta R(\omega)/R(\omega)$. This is often the quantity that is measured directly in non-equilibrium pump probe experiments and is included here for convenience. Considering the top frame first, we see significant differences in the value of $\omega\sigma_2'(\omega)$ for frequencies ω below the gap $\Delta_0 = 24$ meV. In particular, a peak which does not exist in the solid gray curve for the equilibrium case develops in both, the T^* and the μ^* -model. The dotted and dash-dotted curves apply to the μ^* -model without and with change in the gap included while the solid and dashed curves are for the T^* -model. The theory predicts a sharper peak which forms at smaller energy for μ^* as compared with the T^* -model. The center frame of Fig. 3 gives the reflectance $R(\omega)$ vs ω for five cases as in the other frames. As in the top frame, the largest differences in this set of curves occur at frequencies below the gap $\omega < 24$ meV. In that case the T^* -model (solid black and dashed curves without and with the non-equilibrium change in the gap included) predicts a very rapid drop in $R(\omega)$ at the lowest values of ω and then a plateau before a second rapid drop which sets in around the gap. The curve for the μ^* -model, dotted and dash-dotted without and with gap change, is in comparison more structured and in fact shows a small peak in the region 10 to 15 meV. The bottom frame of Fig. 3 serves to emphasize these differences even more. What is plotted is the difference between non-equilibrium and equilibrium value of $R(\omega)$ normalized to this equilibrium value. The quantity $-\delta R(\omega)/R(\omega)$ shows a very rapid rise out of $\omega = 0$ which is larger for the T^* model than for the μ^* -model (by roughly a factor of four). After a maximum is reached, a minimum is seen only in the μ^* case which shows a second maximum within the gap region (corresponding to the structures in the conductivity in the top frame of Fig. 2 at $\Delta_0 - \mu^*$) before the change in reflectance becomes quite small. In both models the region between Δ_0 and $2\Delta_0$ is also affected and is quite sensitive to changes in the gap value.

We have carried out additional calculations for values of c in the impurity potential away from the Born limit. Here we report only one case. In Fig. 4 we show results for $\Delta_0 = 24$ meV, as in a previous figure with $T = 3$ K, $\Gamma^+ = 0.01$ meV and $c = 0.2$ which is near the unitary limit. What is shown in the top frame is the reflectance as a function of frequency. The gray curve is the equivalent equilibrium case included for comparison. The dashed curve is based on the T^* -model and the dash-dotted curve on the μ^* -model. The middle frame gives the corresponding results for the real part of the optical conductivity. Comparison of these results with the equivalent results shown in the bottom frame of Fig. 2 reveals that the Born limit is a better case in which to investigate non-equilibrium effects in the sense that, for the same non-equilibrium quasiparticle density n the effects are less pronounced for the $c = 0.2$ case.

IV. SIMPLE ANALYTIC RESULTS

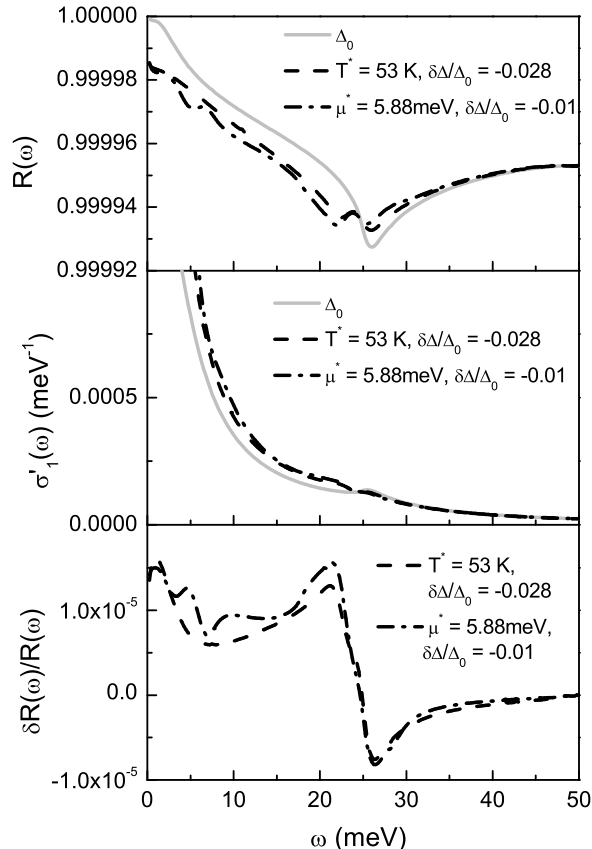


FIG. 4: Reflectance $R(\omega)$ (top frame), real part of the optical conductivity $\sigma'_1(\omega)$ (middle frame), and normalized reflectance difference $\delta R(\omega)/R(\omega)$ (bottom frame) vs ω for a case with $\Delta_0 = 24$ meV, $T = 3$ K, $\Gamma^+ = 0.01$ meV, and $c = 0.2$ near the unitary limit. The gray curve in each of the top two frames is the equilibrium case shown for comparison. The dashed curve is for the T^* -model and the dashed-dotted curve for the μ^* -model.

In contrast to the Born limit, the $\sigma'_1(\omega)$ vs ω (solid gray curve) is now much closer to the non-equilibrium results (dashed or dash-dotted curves). The normalized difference $\delta R(\omega)/R(\omega)$ vs ω is shown in the bottom frame of Fig. 4. The differences between the T^* -model (dashed curve) and the μ^* -model (dash-dotted curve) are less pronounced than was found in the bottom frame of Fig. 3. In our previous analysis of the optical conductivity of various cuprates we have found, in several cases, the need to include in our calculations some impurity scattering in the unitary limit.^{14,32} On the other hand, in some of the very pure samples grown in BaZnO_3 crucibles the mean free path at low temperatures is found to be of the order of a micron and a value of $c \neq 0$ is needed.³¹

It is possible and instructive to derive some simple analytical results for the non-equilibrium conductivity calculated numerically in the previous section. This can provide insight into the physics involved as it makes explicit the dependence on excess quasiparticle density n of various quantities. In terms of the London penetration depth $\lambda_L^{-2}(0)$ the penetration depth in the pure limit at finite temperature and finite μ^* is given by

$$\lambda_L^{-2}(T, \mu^*) = \lambda_L^{-2}(0) \left[1 + \int dE N(E) \frac{\partial f_T(E - \mu^*)}{\partial E} \right], \quad (5)$$

where $N(E)$ is the quasiparticle density of states. For small μ^* at zero temperature the thermal factors in Eq. (5) become a δ -function; we can also use the nodal approximation for $N(E) = E/\Delta_0$ and get immediately

$$\lambda_L^{-2}(0, \mu^*) = \lambda_L^{-2}(0) \left[1 - \frac{\mu^*}{\Delta_0} \right] = \lambda_L^{-2}(0) \left[1 - \sqrt{2n} \right]. \quad (6)$$

The London penetration depth at zero temperature is increased by the presence of a non-equilibrium distribution and the reduction in superfluid density follows a square root of n law. This is also seen in the results presented in the top frame of Fig. 3. A similar result also holds for the T^* model. From Eq. (5) with $\mu^* = 0$ and T replaced by T^* we get

$$\begin{aligned} \lambda_L^{-2}(T^*, \mu^*) &= \lambda_L^{-2}(0) \left[1 - \frac{2 \ln 2}{\Delta_0} T^* \right] \\ &= \lambda_L^{-2}(0) \left[1 - \frac{2 \ln(2) \sqrt{12n}}{\pi} \right]. \end{aligned} \quad (7)$$

The intermediate formula in (7) is just the well known linear in T law for a pure d -wave superconductor. The coefficient of the \sqrt{n} term in the last expression in (7) is 1.53 while in the μ^* -model the coefficient was 1.4. For the same non-equilibrium density n the superfluid density is less reduced from its equilibrium value in the μ^* -model. This mirrors but is the opposite of what was found for the superconducting gap. In both models the reduction follows a $\sqrt{n^3}$ law with coefficients 1.9 in the μ^* -model as compared with 5.4 in the T^* -model. The physics of the reduction in this case is that the states around the Fermi surface occupied by the excess quasiparticles more effectively block the formation of the condensate in the μ^* -model than they do in the T^* -model where they are distributed over higher energy states. Formulas including finite temperature corrections are derived in the Appendix.

In the limit of weak scattering, i.e. $\Gamma^+ \rightarrow 0$ (temperature dominated regime), self consistency is not required in Eq. (4) where $\tilde{\omega}$ on the right hand side can simply be replaced by ω . This corresponds to the temperature dominated regime with $\gamma \ll T$. Here γ is the impurity

scattering rate in the superconducting state and is frequency dependent. Considerable simplifications result as seen in the work of Hirschfeld *et al.*²⁷ Generalizing their result for $0 < \gamma \ll T$ to the non-equilibrium case, the real part of the conductivity is given by

$$\sigma_1(T, \omega) \simeq \frac{\Omega_p^2}{4\pi} \int_{-\infty}^{\infty} d\nu \left(-\frac{\partial f_T(\nu - \mu^*)}{\partial \nu} \right) N(\nu) \times \Im \frac{1}{\omega - i\tau^{-1}(\nu)} \quad (8)$$

where the scattering rate $\tau^{-1}(\omega) = \gamma(\omega) = -\Im \tilde{\omega}(\omega + i0^+)$ is to be determined by Eq. (4) with $\tilde{\omega}$ replaced by ω on the right hand side. The result for a general value of c is

$$\tau^{-1}(\omega) = \pi\Gamma^+ \frac{\omega}{\Delta_0} \frac{c^2 + A_+(\omega)}{c^4 + 2c^2 A_-(\omega) + A_+^2(\omega)}, \quad (9)$$

where

$$A_{\pm}(\omega) = \left(\frac{2\omega}{\pi\Delta_0} \right)^2 \left[\left(\frac{\pi}{2} \right)^2 \pm \ln^2 \left(\frac{2\Delta_0}{\omega} \right) \right]. \quad (10)$$

Two limits are normally considered. The Born limit with $c \rightarrow \infty$ and the unitary limit with $c = 0$. In these limits we get:

$$\tau^{-1}(\omega) = \begin{cases} \frac{\pi^3 \Gamma^+}{4} \frac{\Delta_0}{\omega} \frac{1}{(\pi/2)^2 + \ln^2(2\Delta_0/\omega)} & c = 0 \\ \frac{\pi\Gamma^+}{c^2} \frac{\omega}{\Delta_0} & c \rightarrow \infty. \end{cases} \quad (11)$$

In this last equation we can write $\pi\Gamma^+ = n_I/[\pi N(0)]$ and making use of the relation $c^{-1} = 2\pi N(0)V_{imp}$, we get $\pi\Gamma^+/c^2 = 2\Gamma_B$ with $\Gamma_B = 2\pi n_I N(0)V_{imp}^2$, the well known formula for impurity scattering (Fermi Golden Rule). We can now use the scattering rates in the conductivity formula (8).

We begin with the μ^* -model. For small temperatures $\ll \mu^*$, ($\gamma \ll T \ll \mu^*$)

$$\sigma_1(T, \omega) = \frac{\Omega_p^2}{4\pi} \frac{\mu^*}{\Delta_0} \frac{\tau(\mu^*)}{1 + \omega^2 \tau^2(\mu^*)}. \quad (12)$$

The finite frequency conductivity samples only the scattering time at the single frequency $\nu = \mu^*$ in this model. They are

$$\tau^{-1}(\mu^*) = \begin{cases} \frac{\pi^3 \Gamma^+}{4} \frac{1}{\sqrt{2n}} \frac{1}{(\pi/2)^2 + \ln^2(\sqrt{2/n})}, & c = 0 \\ 2\Gamma_B \sqrt{2n}, & c \rightarrow \infty. \end{cases} \quad (13)$$

We see that in the Born limit $\tau^{-1}(\mu^*)$ is directly proportional to the square root of the excess quasiparticle density, while it varies as its inverse in the unitary limit with some other additional, weaker logarithmic dependence on the square root of n . This means that the half width of the microwave conductivity will be strongly affected by changes in n and that the effects will be opposite in Born

and unitary limit. These features are directly related to the details of the quasiparticle density of states at small ω in a d -wave superconductor and $\tau^{-1}(\mu^*)$ as a function of μ^* gives this information directly.

From Eq. (12) one can easily compute the spectral optical weight remaining under σ_1 . We define A as

$$A = \int_0^{\infty} d\omega \sigma_1(\omega) = \frac{\Omega_p^2}{8} \frac{\mu^*}{\Delta_0} = \frac{\Omega_p^2}{8} \sqrt{2n}, \quad (14)$$

which gives a square root of n law independent of Born or unitary limit and of temperature, but the restriction $\gamma \ll T \ll \mu^*$ must be noted. This accounts exactly for the missing superfluid density brought about by the excess quasiparticles.

In the top frame of Fig. 5 we compare results based on the approximate Eq. (12) with full numerical results based on the exact expression (2). The same impurity parameters as presented in Fig. 2 are used, namely $t^+ = 0.1$ meV with a gap $\Delta_0 = 24$ meV and $T = 3$ K. Several values of the non-equilibrium chemical potential μ^* are considered: $\mu^* = 0$ (black), $\mu^* = 1.47$ meV (dashed), $\mu^* = 2.94$ meV (dotted), $\mu^* = 4.41$ meV (dash-dotted), and $\mu^* = 5.88$ meV (dash-double dotted). The black curves are results based on Eq. (2) while the open symbols are based on Eq. (12). The frequency ω is restricted to small values below 1.0 meV. We see remarkable agreement between the full theory and Eq. (12). This agreement, of course, will fail as ω is increased outside the validity of the approximation used to derive Eq. (12). This is seen in the bottom frame of Fig. 5 where ω now goes up to 50 meV, i.e. up to about twice the gap value. For this higher frequency region no simple analytic result can be obtained and it is necessary to return to the numerical results of the previous section.

So far, except for Fig. 5, we have emphasized the expected frequency dependence of the optical parameters for a given value of excess quasiparticle density n . The data in Fig. 5 can be replotted to give the conductivity $\sigma_1(\omega, \mu^*)$ at a given frequency ω as a function of μ^* . It is clear from Eqs. (12) and (13) that in the Born limit for $\omega\tau(\mu) \gg 1$, $\sigma_1(T, \omega)$ will be proportional to $(\mu^*)^2$ and inversely proportional to ω^2 . This is shown in the top frame of Fig. 6 where exact numerical results (solid lines) are compared with the approximate results of Eq. (12) (solid symbols). The expected linear variation with the excess quasiparticle density [$n \propto (\mu^*)^2$] is pretty well verified. Since in experiments it is the change in reflectance R which is measured directly we show in the bottom frame of Fig. 6 results of this quantity at five frequencies, again as a function of $n \propto (\mu^*)^2$. These data, based on exact numerical calculations, show that the dependence of $\delta R/R$ on n is not exactly linear.

Similar results to those embodied in Eqs. (8) to (14) for the μ^* -model can be obtained in the T^* model as well. We give only a few analytic results here without comparison to full numerical work. First we note that

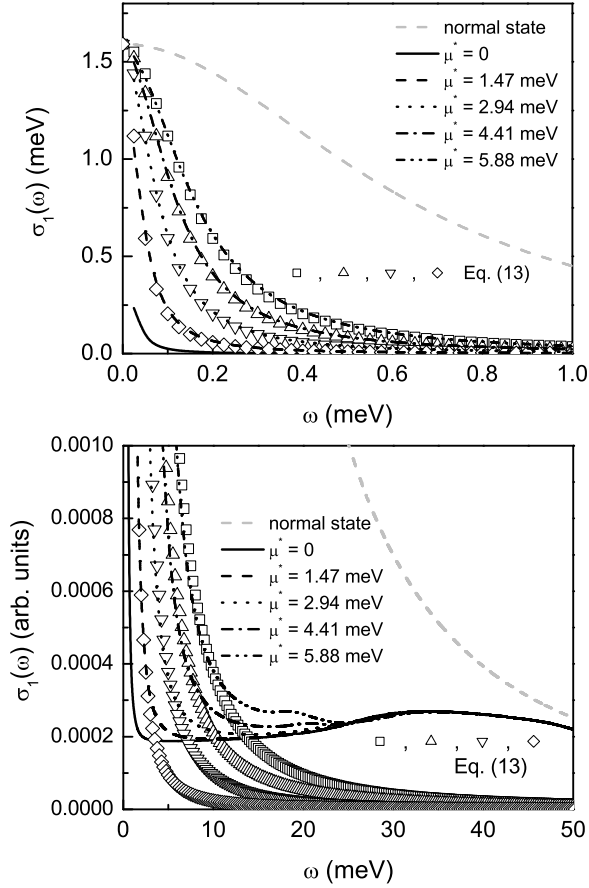


FIG. 5: Comparison of exact results (black lines) for $\sigma_1(T, \omega)$ [Eq. (2)] with the approximate analytic result of Eq. (12) (open symbols). The top frame is for frequencies restricted to $0 \leq \omega \leq 1$ meV while the bottom frame spans to 50 meV. The gray dashed curve is the normal state for $t^+ = 0.1$ meV and $T = 3$ K. The superconducting gap is 24 meV, five values of μ^* are shown.

the residual absorption is

$$A = \frac{\Omega_p^2}{8} \int d\omega \left(-\frac{\partial f_{T^*}(\omega)}{\partial \omega} \right) N(\omega) = \frac{\Omega_p^2}{8} \frac{2 \ln(2)}{\Delta_0} T^* \simeq 1.08 \frac{\Omega_p^2}{8} \sqrt{2n}, \quad (15)$$

which is just the missing superfluid density due to T^* [see Eq. (5)]. The situation is, however, more complicated when the details of the microwave conductivity are considered. A simple form such as Eq. (12) can no longer be derived and we must return to Eq. (8) which gives

$$\sigma_1(\omega) \simeq \frac{\Omega_p^2}{4\pi} \int_{-\infty}^{\infty} d\nu \left(-\frac{\partial f_{T^*}(\nu)}{\partial \nu} \right) \frac{|\nu|}{\Delta_0} \frac{\tau(\nu)}{1 + \omega^2 \tau^2(\nu)}, \quad (16)$$

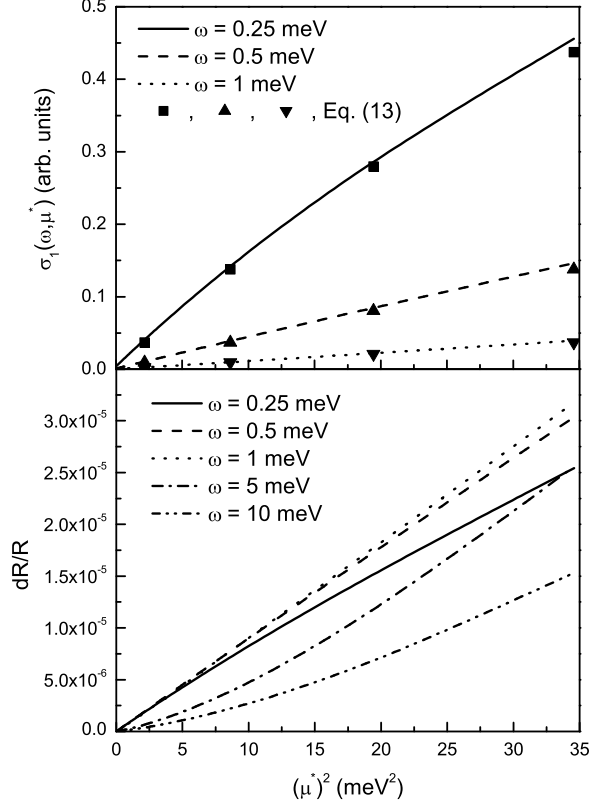


FIG. 6: Top frame: Real part of the conductivity $\sigma_1(\omega, \mu^*)$ at three frequencies $\omega = 0.25, 0.5,$ and 1.0 meV as a function of the square of the chemical potential μ^* ($\sim n$). The lines are based on exact numerical evaluations of Eq. (2) while the solid symbols are based on the approximate analytic formula (12). Bottom frame: The normalized change in reflectivity $\delta R/R$ at five frequencies, $\omega = 0.25, 0.5, 1.0, 5.0,$ and 10.0 meV as a function of $(\mu^*)^2$ ($\sim n$) based on numerical evaluation of Eq. (2). In both frames $\Delta_0 = 24$ meV, $t^+ = 0.1$ meV, and $T = 3$ K.

where the temperature in the Fermi function is T^* rather than T . Even if the frequency ν in the logarithm that occurs in the Eqs. (9) for $\tau(\nu)$ is replaced by T^* , the integral in Eq. (16) cannot be done analytically for a finite value of ω . In effect several values of $\tau(\omega)$ are sampled in Eq. (16) in contrast to the μ^* -model where only $\tau(\mu^*)$ enters. This is a true difference between the two models. If $\omega = 0$, however, we do get an analytic result (assuming $\gamma \ll T \ll T^*$):

$$\sigma(\omega \rightarrow 0) = \begin{cases} \frac{\Omega_p^2}{4\pi} \frac{1}{2\Gamma_B}, & c \rightarrow \infty, \\ \frac{\Omega_p^2}{4\pi} \frac{16n}{\pi^3 \Gamma^+} \left[\left(\frac{\pi}{2} \right)^2 + \ln^2 \left(\frac{\pi}{\sqrt{3n}} \right) \right], & c = 0. \end{cases} \quad (17a)$$

In the opposite limit, ω going to ∞

$$\sigma(\omega) = \begin{cases} \frac{\Omega_p^2}{4\pi} 8n \frac{\Gamma_B}{\omega^2}, & c \rightarrow \infty, \\ \frac{\Omega_p^2}{4\pi} \pi^{-3} \frac{\Gamma^+}{4\omega^2} \frac{1}{(\pi/2)^2 + \ln^2(\pi/\sqrt{3}n)}, & c = 0. \end{cases} \quad (17b)$$

We note that, in both cases, the dependence of the conductivity on the excess quasiparticle density n is very different in the two impurity limits considered. The nature of the impurity scattering is having a profound effect on the optical conductivity. For $\omega \rightarrow 0$ in the Born limit, n drops out of the expression for the conductivity which then takes on its normal state value. For the unitary limit, instead, it goes like $n \ln^2(n)$. For $\omega \rightarrow \infty$ in the Born limit the conductivity is proportional to n and in the unitary limit it varies inversely as $\ln^2(n)$. Similar results hold for the μ^* -model; only the numerical factors are changed as can easily be verified from the general case (12). In particular, the $c \rightarrow \infty$ result of (17a) stays unchanged and the $c = 0$ result is reduced by a factor of two, and the numerical factor in the logarithm $\pi/\sqrt{3} = 1.81$ is reduced by $\sqrt{2} = 1.41$; the $\omega \rightarrow \infty$ result of (17b) is reduced by two and for $c = 0$ we get the same result except for the numerical factor in the logarithm which goes from 1.81 to 1.41. While there are some quantitative differences between the results for the real part of the conductivity between T^* and μ^* -models, in the restricted parameter range in which our analytic results apply, and for $\omega \rightarrow \infty$ the excess quasiparticles dominate the value of the conductivity. The condition $\gamma \ll T \ll T^*$ implies that $\Omega_p^2/(4\pi)(T^*/\Delta_0)^2(2/3)\pi^2(\Gamma_B/\omega^2)$ [which is the result for the Born limit in Eq. (17b)] is much larger than its value when $n = 0$, in which case T replaces T^* in this expression; we note that the condition $T \ll T^*$ has been assumed. The same holds for the unitary limit.

Finally, we consider possible modifications of the so-called universal limit. Applying a nodal approximation to the formula for the $T < \Delta_0$ conductivity, Eq. (2), it reduces at zero frequency³³

$$\sigma_1(T, 0) = \frac{\Omega_p^2}{4\pi} \frac{1}{\pi\Delta_0} \int_{-\infty}^{\infty} d\omega \left(-\frac{\partial f_T(\omega)}{\partial \omega} \right) \times \left[1 + \frac{\omega}{\gamma(\omega)} \tan^{-1} \left(\frac{\omega}{\gamma(\omega)} \right) \right], \quad (18)$$

for $T \rightarrow 0$ this gives $\sigma_1(0, 0) = [\Omega_p^2/(4\pi)][1/(\pi\Delta_0)] \equiv \sigma_{00}$ which is the well known universal limit^{34,35} independent of impurity scattering. Generalization to non-equilibrium in the μ^* -model gives

$$\sigma_1(0, 0) = \frac{\Omega_p^2}{4\pi} \frac{1}{\pi\Delta_0} \left[1 + \frac{\mu^*}{\gamma(\mu^*)} \tan^{-1} \left(\frac{\mu^*}{\gamma(\mu^*)} \right) \right], \quad (19)$$

where $\gamma(\omega) \simeq \gamma[1 + b(\omega/\gamma)^2]$ (with b a constant²⁷) obtained from a self consistent solution of Eq. (4) for small but finite ω . For $\mu^* \ll \gamma$ we can replace $\gamma(\mu^*)$ by its

constant value of γ and find

$$\sigma_1(0, 0) = \sigma_{00} \left[1 + \left(\frac{\mu^*}{\gamma} \right)^2 \right] = \sigma_{00} \left[1 + \left(\frac{\Delta_0}{\gamma} \right)^2 2n \right]. \quad (20)$$

The connection to σ_{00} depends linearly on n and on the inverse square of γ . Universality is lost.

V. CONCLUSION

We have presented results for the modifications of the optical conductivity $\sigma_1(T, \omega)$ that are brought about by introduction of a finite non-equilibrium excess quasiparticle density n . To describe the non-equilibrium distribution in energy, we use two simplified models that have been found to be useful for the s -wave case. While not expected to be accurate the μ^* -model of Owen and Scalapino²¹ and the T^* -model of Parker^{22,23} have the great advantage that the physics involved becomes transparent. The frequency dependent conductivity shows distinct features associated with the chemical potential which should be observable. While both, the μ^* and the T^* -model give similar results qualitatively, there are some important quantitative differences. Numerical results for the real and the imaginary part of σ are given separately, as is the reflectance and the normalized change in reflectance brought about by the excess quasiparticle density. We have also given several analytic results which we hope will prove helpful in the analysis of experimental data.

Acknowledgment

Research supported by the Natural Sciences and Engineering Research Council of Canada (NSERC) and by the Canadian Institute for Advanced Research (CIAR).

APPENDIX A: FINITE TEMPERATURE CORRECTIONS

We consider finite temperatures in the penetration depth. The algebra is simplest in the T^* -model. The thermal quasiparticle density in a d -wave superconductor at temperature T is given by $(\pi^2/12)(T/\Delta_0)^2$ and so the excess non-equilibrium density n in the T^* -model is

$$n = \frac{\pi^2}{12} \left[\left(\frac{T^*}{\Delta_0} \right)^2 - \left(\frac{T}{\Delta_0} \right)^2 \right]. \quad (A1)$$

Thus, we have

$$\frac{T^*}{\Delta_0} = \sqrt{\frac{12n}{\pi^2} + \left(\frac{T}{\Delta_0} \right)^2}, \quad (A2)$$

which reduces to the known result $T^*/\Delta_0 = 2\sqrt{3n}/\pi$ for $T = 0$.

It is easy to work out the small T correction

$$\frac{T^*}{\Delta_0} = \frac{2\sqrt{3}}{\pi}\sqrt{n} + \frac{\sqrt{3}}{12}\frac{\pi}{\sqrt{n}}\left(\frac{T}{\Delta_0}\right)^2, \quad (\text{A3})$$

while the small n correction to finite T is

$$\frac{T^*}{\Delta_0} = \frac{T}{\Delta_0} + \frac{6n}{\pi^2}\frac{\Delta_0}{T}. \quad (\text{A4})$$

Equation (A3) is valid for $12n/\pi^2 > (T/\Delta_0)^2$ and (A4) for $12n/\pi^2 < (T/\Delta_0)^2$. In (A3) the correction goes like T^2 and is inversely dependent on \sqrt{n} while in (A4) it is linear in n and inversely dependent on temperature. The reduction in gap value due to the non-equilibrium density n also has a temperature dependence which is

$$\frac{\delta\Delta(n)}{\Delta_0} = -4\left\{\left[\frac{12n}{\pi^2} + \left(\frac{T}{\Delta_0}\right)^2\right]^{3/2} - \left(\frac{T}{\Delta_0}\right)^3\right\}, \quad (\text{A5})$$

which reduces to the known result $-32\sqrt{(3n)^3}/\pi^3$ at $T = 0$. It is easy to work out the lowest order T correction to this result as well as at finite T , the lowest order n correction. As these corrections come in as higher order effects in the penetration depth we will not give the expressions here.

The penetration depth follows directly from Eq. (7) with T^* replaced by Eq. (A2). This gives

$$\frac{1}{\lambda_L^2(T^*, T)} = \frac{1}{\lambda_L^2(0)} \left[1 - 2\ln(2)\sqrt{\frac{12n}{\pi^2} + \left(\frac{T}{\Delta_0}\right)^2}\right]. \quad (\text{A6})$$

For $T/\Delta_0 < \sqrt{12n/\pi^2}$ (small T correction) we get the first correction for temperature

$$\frac{1}{\lambda_L^2(T^*, T)} = \frac{1}{\lambda_L^2(0)} \left[1 - \frac{\ln(2)}{\pi}\sqrt{3n} - \frac{\pi\ln(2)}{2\sqrt{3n}}\left(\frac{T}{\Delta_0}\right)^2\right], \quad (\text{A7})$$

and for $T/\Delta_0 > \sqrt{12n/\pi^2}$ (small n correction) the first correction for non-equilibrium to temperature T is

$$\frac{1}{\lambda_L^2(T^*, T)} = \frac{1}{\lambda_L^2(0)} \left[1 - 2\ln(2)\frac{T}{\Delta_0} - \frac{12\ln(2)}{\pi^2}n\frac{\Delta_0}{T}\right], \quad (\text{A8})$$

which follows directly from Eqs. (A3) and (A4). We see from Eq. (A7) that the low temperature behavior of the penetration depth has changed from a T to a T^2 law through the presence of the non-equilibrium density n . This is analogous to the effect of impurities which also bring about a T to T^2 law change at low T . Of course, at higher values of T we recover a linear in T law as is indicated in Eq. (A8) with a small correction for the non-equilibrium density n .

A similar situation holds in the μ^* -model but the algebra is not as tidy and we will only give two results. It is easy to work out the finite temperature correction to the chemical potential. From its definition (A1)

$$\begin{aligned} n\Delta_0 &= \int_0^{\mu^*} dE \frac{E}{\Delta(0)} f_T(E - \mu^*) + \int_0^{\infty} dE f_T(E) \\ &= \frac{\mu^{*2}}{2\Delta_0} + \frac{\mu^*}{\Delta_0} T^2 \ln(2). \end{aligned} \quad (\text{A9})$$

The solution for μ^*/Δ_0 is

$$\frac{\mu^*}{\Delta_0} = -2\ln(2)\frac{T}{\Delta_0} + \sqrt{2n + \left(\frac{2T\ln(2)}{\Delta_0}\right)^2}, \quad (\text{A10})$$

which properly reduces to $\sqrt{2n}$ at $T = 0$ and to zero for $n = 0$. For $\mu^*/T \rightarrow \infty$ the expression for λ_L^{-2} remains that given Eq. (6), and we get

$$\frac{1}{\lambda_L^2(T^*, T)} = \frac{1}{\lambda_L^2(0)} \left[1 - \sqrt{2n + \left(\frac{2T\ln(2)}{\Delta_0}\right)^2}\right], \quad (\text{A11})$$

and the square bracket reduces to $1 - \sqrt{2n}$ at $T = 0$ and shows a positive leading, linear in temperature correction with the slope half the value it would have in the equilibrium case. This is different from the T^* -model and is due to the very different non-equilibrium thermal distribution employed in the models which shows up at very small T . At large T , the μ^* -model gives

$$\frac{1}{\lambda_L^2(T^*, T)} = \frac{1}{\lambda_L^2(0)} \left[1 - 2\ln(2)\frac{T}{\Delta_0} + \frac{n}{2T}\Delta_0\right], \quad (\text{A12})$$

which is the same as Eq. (A8) except for a slightly different numerical coefficient in the last term 0.5 rather than 0.8.

* Electronic address: schachinger@itp.tu-graz.ac.at; URL: www.itp.tu-graz.ac.at/~ewald

¹ *Nonequilibrium Superconductivity*, ed. D.N. Langenberg and A.I. Larkin, North-Holland (New York, 1986).

² N. Kopnin, *Theory of Nonequilibrium Superconductivity*, Clarendon Press (Oxford, 2001).

³ A.M. Julian and G.F. Zharkov, *Nonequilibrium Electrons*

and Phonons in Superconductors, Plenum (New York, 1999).

⁴ W.N. Hardy, D.A. Bonn, D.C. Morgan, R. Liang, and K. Zhang, Phys. Rev. Lett. **70**, 3999 (1993).

⁵ Z.-X. Shen, D.S. Dessau, B.O. Wells, D.M. King, W.E. Spicer, A.J. Arko, D. Marshall, L.W. Lombardo, A. Kapitulnik, P. Dickinson, S. Doniach, J. DiCarlo,

- A.G. Loeser, and C.H. Park, Phys. Rev. Lett. **70**, 1553 (1993).
- ⁶ D.A. Wollmann, D.J. Van Harlingen, W.C. Lee, D.M. Ginsberg, and A.J. Legett, Phys. Rev. Lett. **71**, 2134 (1993).
- ⁷ C.C. Tsuei, J.R. Kirtley, C.C. Chi, LockSeeYu-Jahnes, A. Gubta, T. Shaw, J.Z. Sun, and M.B. Ketchen, Phys. Rev. Lett. **73**, 593 (1994).
- ⁸ P.B. Allen, Phys. Rev. Lett. **59**, 1460 (1987).
- ⁹ J.P. Carbotte, E. Schachinger, and D.N. Basov, Nature (London) **401**, 354 (1999).
- ¹⁰ E. Schachinger and J.P. Carbotte, Phys. Rev. B **62**, 9054 (2000).
- ¹¹ E. Schachinger, J.P. Carbotte, and D.N. Basov, Europhys. Lett. **54**, 380 (2001).
- ¹² E. Schachinger and J.P. Carbotte, Physica C **364**, 13 (2001).
- ¹³ E. Schachinger and J.P. Carbotte, in: *Models and Methods of High-TC Superconductivity: some Frontal Aspects, Vol. II*, ed.: J.K. Srivastava and S.M. Rao, Nova Science, Hauppauge NY (2003), pp. 73.
- ¹⁴ E. Schachinger and J.P. Carbotte, J. Phys. Studies (L'viv, Ukraine) **7**, 209 (2003);
- ¹⁵ P. Monthoux and D. Pines, Phys. Rev. B **47**, 6069 (1993); Phys. Rev. B **49**, 4261 (1994); Phys. Rev. B **50**, 16015 (1994).
- ¹⁶ B.J. Feenstra, J. Schützmann, D. van der Marel, R. PerezPinaya, and M. Decroux, Phys. Rev. Lett. **79**, 4890 (1997).
- ¹⁷ V.V. Kabanov, J. Demsar, B. Podobnik, and D. Mihailovic, Phys. Rev. B **59**, 1497 (1999).
- ¹⁸ G.L. Carr, R.P.S.M. Lobo, J. LaVeigne, D.H. Reitze, and D.B. Tanner, Phys. Rev. Lett. **85**, 3001 (2000).
- ¹⁹ R.A.M. Woerner, T. Elsaesser, W.C. Smith, J.F. Ryan, G.A. Farman, M.P. McCurry, and D.G. Walmsley, Science **287**, 470 (2000).
- ²⁰ E.J. Nicol and J.P. Carbotte, Phys. Rev. B **67**, 214506 (2003).
- ²¹ C.S. Owen and D.J. Scalapino, Phys. Rev. Lett. **28**, 1559 (1972).
- ²² W.H. Parker and W.D. Williams, Phys. Rev. Lett. **29**, 924 (1972).
- ²³ W.H. Parker, Phys. Rev. B **12**, 3667 (1975).
- ²⁴ J.J. Chang and D.J. Scalapino, Phys. Rev. B **9**, 4769 (1974).
- ²⁵ D.C. Mattis and J. Bardeen, Phys. Rev. **111**, 412 (1958).
- ²⁶ I. Schürerer, E. Schachinger, and J.P. Carbotte, Physics C **303**, 287 (1998); J. Low Temp. Phys. **115**, 251 (1999).
- ²⁷ P.J. Hirschfeld, W.O. Putikka, and D.J. Scalapino, Phys. Rev. B **50**, 10 250 (1994).
- ²⁸ F. Marsiglio and J.P. Carbotte, Aust. J. Phys. **50**, 975 (1997); Aust. J. Phys. **50**, 1011 (1997).
- ²⁹ F. Marsiglio and J.P. Carbotte, in: *the physics of Superconductors: Conventional and High T_c Superconductors*, eds. K.H. Bennemann and J.B. Ketterson, pp. 233-345, Springer (2003).
- ³⁰ P.J. Hirschfeld and N. Goldenfeld, Phys. Rev. B **48**, 4219 (1993).
- ³¹ E. Schachinger and J.P. Carbotte, Phys. Rev. B **65**, 064514 (2002).
- ³² E. Schachinger and J.P. Carbotte, Phys. Rev. B **64**, 094501 (2001);
- ³³ Wonkee Kim and J.P. Carbotte, Phys. Rev. B **66**, 033104 (2002).
- ³⁴ P.A. Lee, Phys. Rev. Lett. **71**, 1887 (1993).
- ³⁵ W.C. Wu, D. Branch, and J.P. Carbotte, Phys. Rev. B **58**, 3417 (1998).